Supplementary Materials and Methods

Energy Balance

Irrespective of surgical type, mice lose from 15% to 30% of their preoperative body weight as a result of perioperative stress as measured at the end of postoperative week 1. After recovery and resumption of ad libitum feeding, RYGB mice regain weight at a substantially reduced rate compared with sham mice (Supplementary Figure 1*C*). To control for inter-animal variability in immediate postoperative weight loss in experiments involving the MC4R models, mice were weight-matched by calorie restriction on the last few days of postoperative recovery. This ensured that differences in measures of energy balance and body weight observed by week 6 were caused exclusively by RYGB-induced differences in energy balance, enabling a more accurate comparison of effects of RYGB across genotype. A group of DIO mice was generated in parallel as a positive control for RYGB-induced weight reduction using this methodology. RYGB-induced body weight reduction was equivalent whether compared with conventional sham mice or sham mice that were weight-matched at the end of recovery (Supplementary Figure 3).

Body weight and food intake were measured daily from the first day of postoperative recovery through week 6. Body composition was measured on resumption of ad libitum feeding and after body weight plateau. Stool was collected, dried, weighed on a daily basis, and analyzed using bomb calorimetry (University of Arkansas Center of Excellence for Poultry Science). Gain in body mass energy was calculated using values of 37.7 kJ/g fat mass and 4.2 kJ/g fat-free-mass. Metabolic efficiency represents a gain in mass energy expressed as a percentage of total intake; feeding efficiency is weight gain per kilojoule consumed. To adjust for stool energy losses, total intake was multiplied by the percentage of total calorie absorption. For estimating basal energy expenditure, the energetic cost of depositing fat mass and lean mass was estimated using values of 55.3 and 9.2 kJ/g, respectively, as previously described.[1–3] Supplementary Table 1 shows measures of energy balance.

HFD Challenge

MC4R-null and MC4R-Het mice maintained on regular chow before and after surgery were challenged with HFD during week 8. Body weight, food intake, and stool output were measured daily during the acute challenge (8 days) and weekly during the extended challenge (3 weeks). MC4R-Het mice and a subcohort of MC4R-null mice were killed after acute challenge; a subcohort of MC4R-null mice also was killed after extended challenge.

Glucose Homeostasis

Glucose homeostasis was evaluated between weeks 6 and 8 to avoid confounding by postoperative weight loss owing to perioperative stress and calorie restriction and the ensuing convalescence. Sham animals typically recover their preoperative weight by week 4, representing the end of this convalescent period; experiments before this time therefore are confounded by the metabolic effects of recovery (Supplementary Figure 1*C*). To further circumvent this issue, glucose homeostasis was evaluated in CRWM-sham mice to control for antidiabetic effects of postoperative calorie restriction and weight loss.

Basal. The blood glucose level was measured from the tail vein using a hand-held glucometer (Bayer Healthcare, Tarrytown, NY). Plasma samples were collected from the tail vein. Mice were fasted overnight from the start of the dark cycle (18:00). HOMA-IR, a mathematic model approximating treatment effects on insulin resistance and validated in humans and rodents,[4] was calculated as previously described.

Glucose tolerance. In fasted mice, the blood glucose level was measured before and at the indicated times after administration of 1 g/kg D-glucose (Sigma-Aldrich, St. Louis, MO) by oral gavage. Plasma was collected before and at 15 and 30 minutes during the oral glucose tolerance test to measure glucose-stimulated insulin.

Insulin tolerance. Four-hour fasted mice (09:00–13:00) were administered 0.75 U/kg insulin (Eli Lilly, Indianapolis, IN) by intraperitoneal injection and blood glucose level was measured before and at the indicated times after injection.

Peripheral glucose uptake. In brief, fasted mice were administered a 1 g/kg body weight bolus of D-glucose containing 2-deoxy-D-[1-^{3}H] glucose at 0.5 uci/g body weight (Amersham Pharmacia Biotech, Piscataway, NJ) by oral gavage. Blood glucose level was measured from tail vein blood using a hand-held glucometer. Additional blood was collected into EDTA, and skeletal muscle (gastrocnemius and soleus) and white adipose tissue (gonadal) were collected 30 minutes after gavage. Radioactivity was measured using a LS6500 Multipurpose Scintillation Counter (Beckman Coulter, Brea, CA). Glucose-specific activity (in degenerations per minute per micromole) was calculated by dividing sample radioactivity by the glucose concentration, and area under the curve was integrated for the duration of the experiment. To calculate 2-deoxy-glucose uptake, the counts (degenerations per minute) were divided by the integrated glucose-specific activity area under the curve and the sample protein content.

Pyruvate tolerance. In fasted mice, the blood glucose level was measured before and at the indicated times after intraperitoneal injection of 2 g/kg sodium pyruvate (Sigma-Aldrich, St. Louis, MO). As a control for phosphoenolpyruvate carboxykinase-dependent glucose production, mice were pretreated with 30 mg/kg of the phophoenolpyruvate carboxykinase inhibitor 3-mercaptopicolinic acid (Toronto Research Chemicals, Toronto, Ontario, Canada) by oral gavage 30 minutes before sodium pyruvate injection.

Blood and Tissue Chemistries

Leptin (University of Texas Southwestern Mouse Metabolic Phenotyping Center) and triglyceride (Yale Mouse Metabolic Phenotyping Center) levels were mea-

sured in fasting serum. Plasma insulin was measured using a high sensitivity mouse insulin enzyme-linked immunosorbent assay (Crystal Chem, Downers Grove, IL). Tissue triglyceride levels were measured from frozen liver or skeletal muscle tissue using colorimetry (University of Texas Southwestern Mouse Metabolic Phenotyping Center).

Metabolic Flux Analysis

Tracer delivery. Mice were implanted surgically with an indwelling jugular vein catheter and allowed to recover for 5 days. After an overnight fast (~16 h), mice received an intraperitoneal injection of isotonic solution of D_2O (99%; 28 μL/g body weight). Immediately after the injection, [U-$^{13}C_3$] propionate (50 mg/mL) and [3, 4-$^{13}C_2$] glucose (3.72 mg/mL) were administered first as a bolus for the first 10 minutes (6.1 μmol/h) and then as a continuous infusion (1.2 μmol/h) for the next 80 minutes. During this entire period of infusion, mice were allowed unrestrained movement in their cages.

Metabolic analysis by NMR. Plasma glucose was extracted with 0.3 N zinc sulfate, neutralized with 0.3 N barium hydroxide to isolate glucose, which later was converted to the 1,2-isopropylidene glucofuranose derivative (monoacetone glucose) as previously described.[5,6] The ^{2}H and ^{13}C NMR spectra of monoacetate glucose were acquired in a 14-T NMR spectrometer with a 3-mm broadband probe (Varian, Palo Alto, CA) and peak areas (^{2}H and ^{13}C) were integrated using the 1D NMR software ACD/Labs 9.0 (Advanced Chemistry Development Toronto, Ontario, Canada) as previously described.[5,6] Endogenous glucose production, glycogenolysis, and gluconeogenesis were determined as previously described.[5,6]

Insulin Signaling and Western Blots

Tissue samples were harvested from overnight fasted mice at baseline or after 4 minutes of insulin stimulation via the inferior vena cava. Whole-cell lysates were prepared by homogenization in ice-cold sodium dodecyl sulfate–lysis buffer (10 mmol/L Tris-HCl, pH 6.8, 1% sodium dodecyl sulfate, 100 mmol/L NaCl, 1 mmol/L EDTA, 1 mmol/L EGTA, Protease Inhibitor Tablets [Roche, Indianapolis, IN], phosphatase inhibitor cocktail [EMD Millipore, Billerica, MA]). Aliquots were subjected to immunoprecipitation using IRS1 (EMD Millipore) or IRS2 antibodies (EMD Millipore). Denatured cell lysates and immunoprecipitates were collected on protein-A sepharose, separated on precast sodium dodecyl sulfate–polyacrylamide gel electrophoresis denaturing gradient gels (Bio-Rad), and subjected to Western blotting after transfer to nitrocellulose. Antisera against antiphosphotyrosine (EMD Millipore), β-actin (Sigma-Aldrich, St. Louis, MO), IRS1, and IRS2 were used for immunoblotting and detected via enhanced chemiluminescence (Amersham Pharmacia Biotech, Piscataway, NJ).

Human Data

A cohort of 1433 patients who underwent RYGB at Geisinger Clinic was followed up for 12 months presurgery and up to 48 months after surgery. A lean cohort of 451 age- and sex-matched subjects was selected from the MyCode population at Geisinger Clinic.[19] Both populations and the presurgery and postsurgical care for the RYGB patients have been described in detail elsewhere.[7] The DNA was isolated from blood by Geisinger Clinic Genomic Core and provided for this study in a de-identified manner. The clinical variables as well as weight and height measurements for the coded samples were obtained from a data broker who was not part of the study and did not have access to the genotyping data. By using high-fidelity *Pyrococcus furious* polymerase, the single-exon *MC4R* gene was amplified using 2 primers: MC4R-forward (ATCAATTCAGGGGGACACTG) and MC4R- reverse (TGCATGTTCCTATATTGCGTG). The PCR products were cleaned and analyzed using automated DNA sequencing as described.[8] Body weights at the time of surgery were set at 100% and weights at other times were set accordingly. Body weight curves were best fit using the 4-parameter logistic equation (sigmoidal curve with variable slope):

$$Y = Bottom + \frac{(Top - Bottom)}{1 + 10^{(\log EC_{50} - X) - HillSlope}}$$

Patients typically lose the most weight within 12 months after surgery and achieve a new homeostasis. The slopes of the curves were compared via GraphPad Prism (GraphPad Software, Inc., La Jolla, CA) global fit using F test.

Diabetic patients were identified as those with an hemoglobin A1c level of 6.0 or greater or taking any diabetic medications (biguianides, sulfonylureas, insulin, or insulin-sensitizing agents). Resolution of postsurgery diabetes was assessed based on termination of drug therapy. For the bivariate analysis of mutation rates, the Fisher exact test was used.

Statistical Analysis

All data are presented as mean ± standard error of the mean. Only P values less than .05 were considered statistically significant. For mouse data sets, experiments comparing 2 means were analyzed using the Student t test, with the Welch correction as appropriate. Experiments comparing 3 or more means were analyzed using 1-way analysis of variance (followed by the Tukey–Kramer post hoc) or 2-way analysis of variance (followed by the Bonferroni post hoc) when the experiment involved 2 independent variables. Curves were analyzed using both repeated-measures 2-way analysis of variance and area under the curve analysis using the Student t test or 1-way analysis of variance (followed by the Tukey–Kramer post hoc), where appropriate. The postoperative body weight curve of DIO mice (Supplementary Figure 1*C*) was analyzed using repeated-measures 2-way analysis of variance.

References

1. Rothwell NJ, Stock MJ. A role for brown adipose tissue in diet-induced thermogenesis. Nature 1979;281:31–35.
2. Sutton GM, Trevaskis JL, Hulver MW, et al. Diet-genotype interactions in the development of the obese, insulin-resistant phenotype of C57BL/6J mice lacking melanocortin-3 or -4 receptors. Endocrinology 2006;147:2183–2196.
3. Pullar JD, Webster AJ. The energy cost of fat and protein deposition in the rat. Br J Nutr 1977;37:355–363.
4. Lee S, Muniyappa R, Yan X, et al. Comparison between surrogate indexes of insulin sensitivity and resistance and hyperinsulinemic euglycemic clamp estimates in mice. Am J Physiol Endocrinol Metab 2008;294:E261–E270.
5. Jin ES, Jones JG, Merritt M, et al. Glucose production, gluconeogenesis, and hepatic tricarboxylic acid cycle fluxes measured by nuclear magnetic resonance analysis of a single glucose derivative. Anal Biochem 2004;327:149–155.
6. Burgess SC, Jeffrey FMH, Storey C, et al. Effect of murine strain on metabolic pathways of glucose production after brief or prolonged fasting. Am J Physiol Endocrinol Metab 2005;289:E53–E61.
7. Still CD, Wood GC, Chu X, et al. High allelic burden of four obesity SNPs is associated with poorer weight loss outcomes following gastric bypass surgery. Obesity (Silver Spring) 2011;19:1676–1683.
8. Mirshahi UL, Still CD, Masker KK, et al. The MC4R(I251L) allele is associated with better metabolic status and more weight loss after gastric bypass surgery. J Clin Endocrinol Metab 2011;96:E2088–E2096.

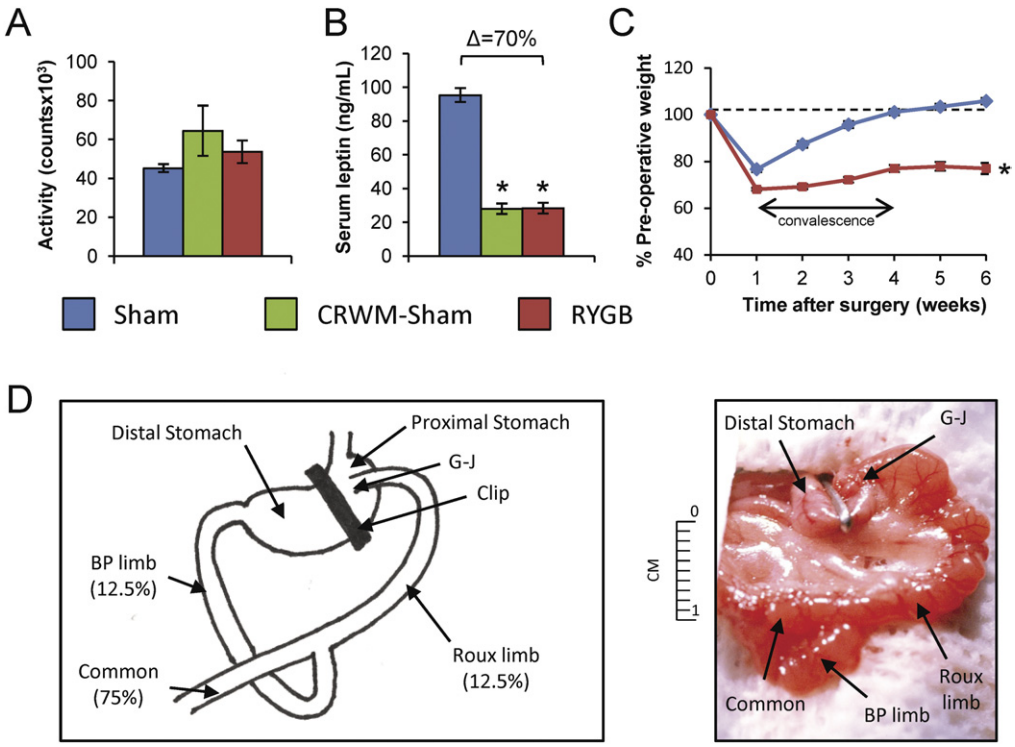

Supplementary Figure 1. RYGB induces weight loss in mice (related to Figure 1). (*A*) Physical activity, as measured during week 5, was unchanged after RYGB (n = 5–6 per group). (*B*) Fasting serum leptin was comparably reduced in RYGB and CRWM-sham mice (n = 9–11 per group). (*C*) Body weight, expressed as a percentage of preoperative weight, was reduced substantially in RYGB-treated DIO mice (red) compared with sham (blue) by postoperative week 1 as a result of perioperative stress and calorie restriction. Acute convalescence ensues for the subsequent 3 weeks because sham-operated mice do not fully regain their preoperative weight until week 4 (RYGB, 27; sham, 29). (*D*) Schematic and photograph of RYGB in mice. After reconstruction, the biliopancreatic (BP) limb and Roux limb each comprise 12.5% of total intestinal length and the common channel (common) comprises 75%. After reconstruction, ingested nutrients pass from the esophagus, through the proximal gastric pouch, and into the Roux limb. Digestive secretions from the excluded gut drain through the BP limb to meet ingested nutrients at the start of the common channel. G-J, gastrojejunal anastomosis. *$P < .05$ vs sham.

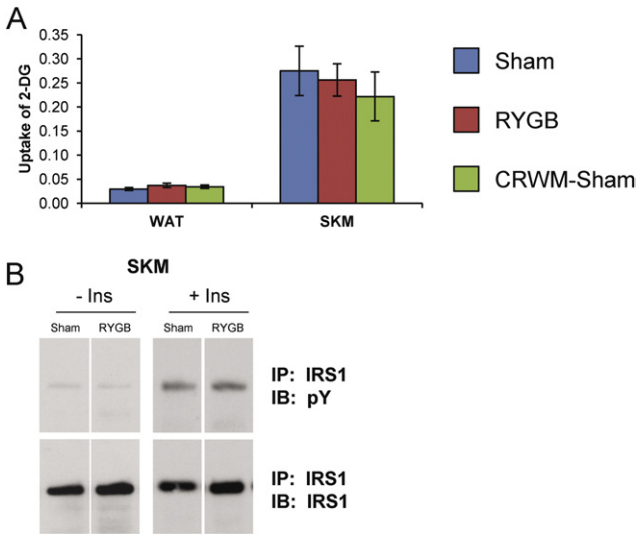

Supplementary Figure 2. RYGB fails to improves glucose homeostasis in skeletal muscle and adipose tissue of DIO mice (related to Figure 2). (*A*) Peripheral glucose uptake into skeletal muscle (SKM) and white adipose tissue (WAT), as measured using 2-deoxy-glucose (2-DG), was unchanged after RYGB (n = 4–5 per group). (*B*) Insulin-stimulated insulin receptor substrate-1 (IRS1) tyrosine phosphorylation and IRS1 expression in SKM was unchanged after RYGB (n = 4 per group).

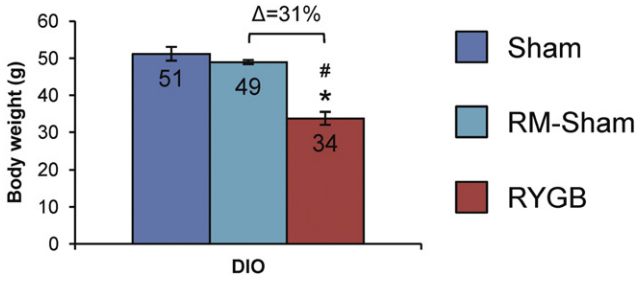

Supplementary Figure 3. RYGB induces equivalent weight loss compared with conventional sham-operated mice and sham-operated mice weight-matched during postoperative recovery (related to Figure 3). To control for differences in susceptibility to perioperative stress (weight loss and calorie restriction) and ensure that the observed differences in energy expenditure and body weight in MC4R models during week 6 were exclusively caused by RYGB-induced differences in energy balance, RYGB-treated and sham-operated mice were weight-matched during postoperative recovery. The group of DIO mice in this figure was generated in parallel with the MC4R mouse models as a positive control for RYGB-induced weight reduction. As seen in this figure, RYGB-treated DIO mice are equivalently weight-reduced by week 6 whether compared with conventional sham-operated mice (provided high-fat diet ad libitum after postoperative recovery; sham) or sham-operated mice that were weight-matched to RYGB-treated mice during recovery (RM-sham) (sham, 4; RM-sham, 6; RYGB, 4). $^{*}P < .05$ vs sham, $^{\#}P < .05$ vs RM-sham.

Supplementary Table 1. Energy Balance Measurements

	DIO		MC4R-null		ChAT-MC4R		Phox-MC4R		MC4R-Het	
	Sham	RYGB	Sham	RYGB	Sham	RYGB	Sham	RYGB	Sham	RYGB
Fat mass, *g*	23.1 ± 1.5	**8.1 ± 1.7**	17.6 ± 0.9	**14.3 ± 1.1**	17.1 ± 0.8	**7.6 ± 0.9**	19.6 ± 1.3	16.0 ± 1.4	13.3 ± 0.6	**4.6 ± 0.5**
Energy intake, *kJ/d*	75.97 ± 1.87	78.02 ± 3.27	68.69 ± 2.23	61.39 ± 2.97	74.17 ± 1.46	**65.00 ± 2.76**	72.43 ± 3.11	67.06 ± 3.36	60.73 ± 1.13	**56.04 ± 1.68**
GBME, *kJ/d*	18.85 ± 1.71	**9.35 ± 2.02**	23.39 ± 1.85	**15.68 ± 1.88**	27.75 ± 2.49	**7.24 ± 2.41**	21.47 ± 3.63	14.16 ± 1.81	21.72 ± 1.40	**7.84 ± 1.65**
FE, *mg/kJ*	6.50 ± 0.55	**3.13 ± 0.68**	9.15 ± 0.69	**6.64 ± 0.51**	9.86 ± 0.74	**2.88 ± 0.94**	8.02 ± 1.44	5.61 ± 0.69	9.45 ± 0.49	**3.74 ± 0.80**
ME%	24.50 ± 2.09	**11.78 ± 2.55**	34.49 ± 2.61	**25.04 ± 1.93**	37.18 ± 2.78	**10.86 ± 3.55**	32.27 ± 4.91	21.17 ± 2.59	35.63 ± 1.84	**14.11 ± 3.00**
FE_{adj}, *mg/kJ*	7.02 ± 0.60	**3.79 ± 0.82**								
$ME\%_{adj}$	26.47 ± 2.26	**14.29 ± 3.10**								

NOTE. Fat mass and energy balance measurements in DIO, MC4R-null, ChAT-MC4R, Phox-MC4R, and MC4R-Het mice after RYGB and sham surgeries. For this experiment, energy intake, fecal energy losses, body composition, and body weight were measured serially from the day of full postoperative recovery during postoperative weeks 2–6. These measures were used to calculate gain in mass energy, metabolic efficiency, and basal energy expenditure as described in detail in the Materials and Methods section. Bolding indicates statistical significance vs sham mice ($P < .05$).

FE, feeding efficiency, daily weight gain per kJ consumed; FE_{adj}, FE adjusted for fecal energy losses, for these calculations, daily energy intake was multiplied by the percentage of total calorie absorption; GBME, gain in body mass energy, energy per gram of fat and lean mass calculated from NMR body composition data using values of 37.7 kJ/g for fat mass and 4.2 kJ/g for lean mass; ME%, metabolic efficiency, gain in mass energy expressed as a percentage of the total intake; $ME\%_{adj}$, ME% adjusted for fecal energy losses, for these calculations, daily energy intake was multiplied by the percentage of total calorie absorption.

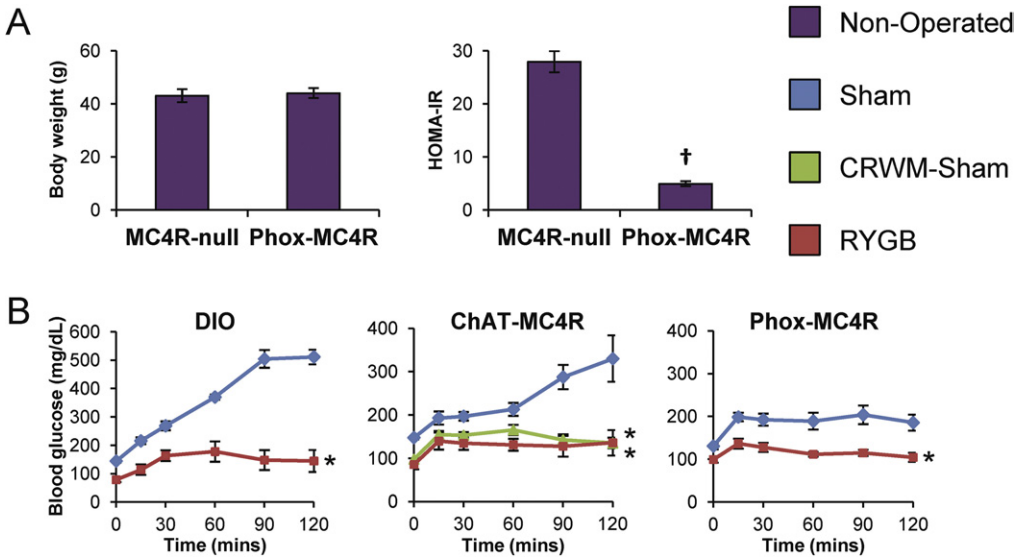

Supplementary Figure 4. RYGB improves glucose homeostasis and pyruvate tolerance in Phox-MC4R and ChAT-MC4R mice (related to Figure 4). (*A*) Despite persistent obesity (*left*), HOMA-IR is reduced in Phox-MC4R mice compared with MC4R-null mice (*right*) (n = 5 per group). (*B*) RYGB reduces glucose excursion after pyruvate administration in DIO, ChAT-MC4R, and Phox-MC4R mice (n = 5–8 per group). *$P < .05$ vs sham, †$P < .05$ vs MC4R-null.

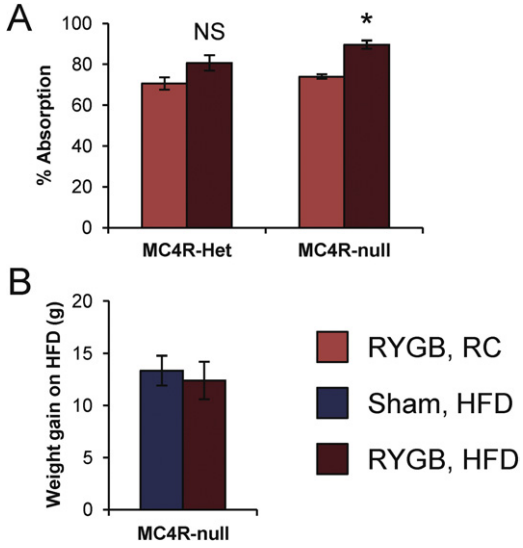

Supplementary Figure 5. RYGB-treated mice are resistant to HFD-induced positive energy balance and weight gain (related to Figure 5). (*A*) Calorie absorption in RYGB-treated MC4R-null and MC4R-Het mice on regular chow (RC) and during acute (8-day) challenge with HFD (n = 5–9 per group). (*B*) Sham- and RYGB-treated MC4R-null mice gained a substantial and equivalent amount of body weight when challenged with HFD for 3 weeks (n = 10–14 per group). *$P < .05$ vs RYGB, RC.

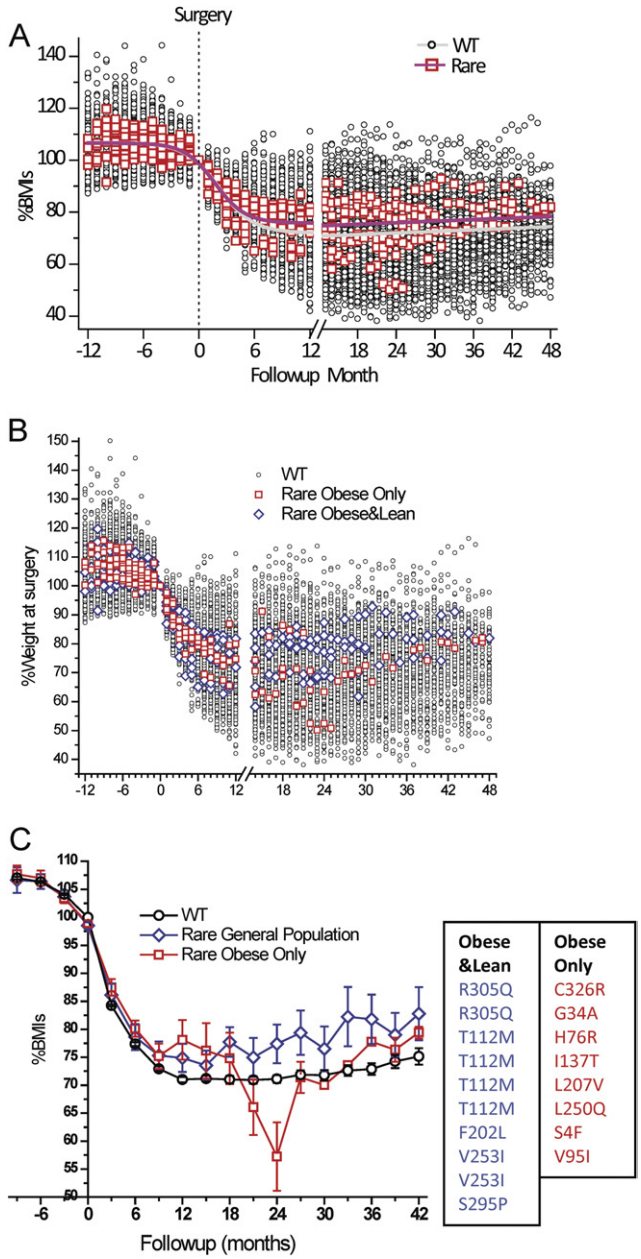

Supplementary Figure 6. RYGB induces equivalent weight loss in carriers and noncarriers of rare *MC4R* variants (related to Figure 6). (*A*) Carriers of rare *MC4R* variants (red, rare) and noncarriers (black, wild type [WT]) show equivalent weight loss after RYGB. The percentage change in body mass index (%BMIs) is shown graphed against the perioperative month; the hashed line at time 0 represents the time of surgery. Purple (carriers) and gray (noncarriers) *lines* represent best-fit curve analysis of change in %BMIs for each group. (*B* and *C*) Because some rare *MC4R* variants have been reported in nonobese subjects, we further subdivided the patients into those carrying variants found only in obese subjects and those variants that have been identified previously in lean and obese patients. (*B*) Weight loss among these 2 groups compared with noncarriers. (*C*) Three-month running average for weight loss in the 3 groups. A list of the rare variants identified in this study is shown in the inset.

Supplementary Table 2. Clinical Parameters at Time of Surgery: Mean ± Standard Error of the Mean

	Wild type	Rare	*P* value[a]
Age, *y*	45.8 ± 0.3 (1353)	44.1 ± 3.0 (18)	.5
Height, *in*	65.6 ± 0.09 (1354)	64.6 ± 0.6 (18)	.2
Hb_{A1C}[b]	5.7 ± 0.02 (628)	5.6 ± 0.1 (8)	.6
Insulin, *μIU/mL*[b]	22 ± 1 (638)	21 ± 6 (9)	.9
Glucose, *mg/dL*[b]	92 ± 1 (663)	85 ± 3 (9)*	.03
HOMA1, arbitrary units[b]	5.3 ± 0.3 (638)	4.3 ± 1 (9)	.4
REE, *kcal/day*	2486 ± 27 (742)	2233 ± 129 (10)	.3
Waist circumference, *in*	53 ± 0.2 (1188)	52 ± 1 (17)	.4
ALT, *U/L*[c]	30 ± 0.7 (856)	39 ± 8 (13)	.3
AST, *U/L*[c]	26 ± 0.5 (853)	32 ± 7 (13)	.5
Alkaline phosphatase, *U/L*[c]	79 ± 0.8 (854)	75 ± 4 (13)	.6
Triglycerides, *mg/dL*[c]	166 ± 3 (855)	162 ± 27 (13)	.9
LDL, *mg/dL*[c]	111 ± 1 (846)	116 ± 7 (13)	.5
Cholesterol, *mg/dL*[c]	190 ± 1 (858)	202 ± 8 (13)	.3
HDL, *mg/dL*[c]	47 ± 0.4 (855)	53 ± 2 (13)**	.008
Cholesterol/HDL ratio[c]	4.2 ± 0.04 (855)	3.8 ± 0.2 (13)	.2

NOTE. Carriers and noncarriers were matched for the indicated parameters.
ALT, alanine aminotransferase; AST, aspartate aminotransferase; HDL, high-density lipoprotein; LDL, low-density lipoprotein; REE, resting energy expenditure.
[a]*P* values from unpaired *t* test between genotypes using the Welch correction for unequal variances whenever necessary. $^{*}P < .05$, $^{**}P < .01$ vs wild-type.
[b]Subjects taking diabetes medicines (biguanides, sulfonylureas, insulin, and insulin-sensitizing agents) were excluded from calculations.
[c]Subjects taking cholesterol absorption medicines (statins) were excluded from these calculations.

Supplementary Table 3. Clinical Parameters at Time of Surgery of the Rare Variants

	Obese and lean	Obese only	*P* value[a]
Age, *y*	46 ± 4 (10)	42 ± 4 (8)	.5
Height, *in*	64 ± 0.6 (10)	65 ± 1 (8)	.5
Hb_{A1C} [b]	5.7 ± 0.1 (5)	5.5 ± 0.2 (3)	.5
Insulin, *μIU/mL*[b]	23 ± 8 (6)	17 ± 8 (3)	.7
Glucose, *mg/dL*[b]	84 ± 4 (6)	86 ± 4 (3)	.8
HOMA1, arbitrary units[b]	4.6 ± 2 (6)	3.7 ± 2 (3)	.7
REE, *kcal/day*	2252 ± 148 (5)	2214 ± 232 (5)	.9
Waist circumference, *in*	53 ± 2 (9)	51 ± 2 (8)	.3
ALT, *U/L*[c]	28 ± 7 (7)	18 ± 4 (5)	.3
AST, *U/L*[c]	22 ± 3 (7)	43 ± 15 (6)	.2
Alkaline phosphatase, *U/L*[c]	70 ± 6 (7)	82 ± 4 (6)	.2
Triglycerides, *mg/dL*[c]	155 ± 42 (7)	171 ± 35 (6)	.8
LDL, *mg/dL*[c]	115 ± 8 (7)	116 ± 13 (6)	1.0
Cholesterol, *mg/dL*[c]	202 ± 8 (7)	202 ± 17 (6)	1.0
HDL, *mg/dL*[c]	55 ± 2 (7)	51 ± 3 (6)	.3
Cholesterol/HDL ratio[c]	4.2 ± 0.04 (855)	3.8 ± 0.2 (13)	.2

NOTE. Carriers of *MC4R* variants were stratified according to association of variants with obese or obese and lean populations. The indicated parameters were matched in both groups at the time of surgery. Rare variants were subdivided based on whether they were identified in subjects from obese cohorts only, or from obese and lean cohorts. Mean ± standard error of the mean (n) is shown.
ALT, alanine aminotransferase; AST, aspartate aminotransferase; HDL, high-density lipoprotein; LDL, low-density lipoprotein; REE, resting energy expenditure.
[a]*P* values from unpaired *t* test between the 2 groups using the Welch correction for unequal variances whenever necessary.
[b]Subjects taking diabetes medicines (biguanides, sulfonylureas, insulin, and insulin-sensitizing agents) were excluded from calculations.
[c]Subjects taking cholesterol absorption medicines (statins) were excluded from these calculations.